Delft University of Technology

Bachelor Thesis

Faculty of Applied Sciences, BSc program "Technische Natuurkunde"
&
Faculty of Electrical Engineering, Mathematics and Computer Science, BSc program "Technische Wiskunde"

Resilience and Synchronization Behaviour within Mean Field Models

Author:
Jesse Mulderij

Supervisors:
Dr. J.L.A. Dubbeldam
Prof. Dr. Y. Blanter

September 25, 2017

Abstract

The study of the dynamics of large, complex networks is generally very hard. Analytical solutions are rarely available and numerical solutions require immense computation times. Recently, Gao et al. [1] have proposed a new theoretical approach to analyse the average behaviour of complex networks. In this research we discuss the derivation of the mean field approximation and the resulting one dimensional, so called, "effective" equation. We offer an alternative derivation. We also give an expression for the error in the form of a differential equation. Applying noise to a model of plants and pollinators uncovers a weak point in the given formalism, the effective equation does not correctly predict the average behaviour of the network. For lower dimensional systems, projecting the synchronization manifold on a phase plot reveals why the mean field approximation works well in the specific case. Finally, the theory is applied to some existing models. First, the Generalized Lotka-Volterra model, where it struggles in specific cases where the network has no stable fixed points but the theory does predict one. Second, the Kuramoto model, where a synchronization state of the oscillators is correctly predicted by the theory, and third, a one dimensional array of Josephson junctions where synchronization is also correctly predicted along with the correct stability criteria.

Contents

Chapter 1

Introduction

The interaction between ports through cargo ship movements [2], the internet [3] and gene regulatory systems [4] are all examples of complex networks. Complex networks consisting of many interacting agents obey hard to derive dynamics that we are far from understanding in full. Currently, the dynamics are generally modeled by relations between pairs of agents in the network, where the strength of interactions between any two agents is denoted by an adjacency matrix. This method is suitable for low dimensional systems with few interacting parts since the computation time becomes a restraining factor as the size of the networks increase. The stability or resilience of complex networks is of rising interest, it tells us the ability of a network to withstand and/or recover from the influence of external perturbations that act upon the system. Human health [5], the economy [6, 7], ecological networks [8] and systems such as the internet [9] are just some of the many fields where the phenomenon of resilience is an open area of research. The collapse of resilience can have detrimental effects on ecological systems -leading to extinction- and economical systems -resulting in economical collapse-,but can rarely be predicted, let alone prevented. Recently, Gao et al. [1] proposed new analytical tools with which to handle large scale complex networks and predict their resilience patterns. Their work consists of a mean field approximation and is based on reducing the multidimensional problem into a 1D, so called, "effective" equation that embodies the entire complex network's dynamics and its stability properties. The topology of the network is summarized by a 1D control parameter. They tested their methods on multiple mutualistic (ie. only positive interactions between pairs of agents are present) networks containing cellular regulation networks, ecological systems and power grids. Tu et al. [10] have shown in response that networks do not need to be mutualistic per se for the method to work. In this report we will review the derivation of Gao et al.'s theory and derive an expression for the error involved with the approximation, we will then highlight some issues with stochastic perturbations and, finally, connect the method to a range of existing models including an array of Josephson junctions and the Kuramoto model. In Chapter 2 the basis of the problem at hand will be mapped out and the derivation of Gao et al. will be presented, after which we will do our own attempt in Chapter 3. In Chapter 4 the connection with Plant-Pollinator ecosystems will be shown. After that, the influence of stochastic perturbations will be analyzed in Chapter 5. Then, in Chapter 6 a steady state analysis ensues for low dimensional systems. Finally, in Chapters 7-9 the framework will be connected to some better known models. First, Lotka-Volterra systems will be discussed briefly. Afterwards, the Kuramoto model and Josephson junctions, two closely related topics, will be analyzed and connected to the theory that Gao et al. provided us with.

Chapter 2

Complex Networks in General

In networks that consist of many non-linearly interacting nodes it is generally very hard to predict the overall behavior. For simple network structures and interactions an analytic solution can sometimes be found. If the networks are more complex (think about ecosystems, transportation networks or particle physics), however, the problem is extremely hard to tackle. Therefore it is useful to have a technique to still be able to determine the behavior of such a network, or at least a good approximation of such behavior. Investigating the stability of large systems is essential to predicting what kind of effect perturbations on these systems will have. Predicting the collapse of plant-pollinator or predator-prey populations, power grids, or the behavior of the alignment of spin particles in solids can be used for a wide range of practical applications.

Lets take a look at an arbitrary network of N nodes that are somehow interacting through some coupling between the nodes. Let us say that the behaviour x_i of node i is governed by some differential equation of the form

$$\dot{x_i} = F_i(x_i) + \sum_j A_{ij} G_i(x_i, x_j) \tag{2.1}$$

where the self-dynamics of x_i are captured in some function $F_i(x_i)$ and the coupling interaction between nodes i and j is determined by a function G_i that depends on both nodes' behaviour. A is an adjacency matrix that captures the coupling strength between two nodes, where the coupling strength of the interaction that x_i undergoes as a result of x_j is given by A_{ij}.

For simplicity we will start by assuming that dynamics do not change per node, that is, every node interacts in the same way ($F_i(x_i) = F(x_i)$, $G_i(x_i, x_j) = G(x_i, x_j)$). This says that every node (e.g. every bee or every particle) acts in the same way if it were in the same situation. This simplification is exact or very precise for many systems we consider in physics. For indistinguishable particles interacting through a pair potential the assumption is perfectly satisfied. There are however a lot of examples where the simplification does not hold at all. If we're dealing with populations of conscious, or even irrationally thinking species, or systems where particles have different masses or charges the assumption gives a very distorted image of reality. Even though this assumption excludes a large amount of interesting systems from this study, we'll have to assume something in order to get anywhere at all. Hence we start from the following simplified equation

$$\dot{x_i} = F(x_i) + \sum_j A_{ij} G(x_i, x_j) \tag{2.2}$$

In this case it seems natural to also assume the matrix A to be symmetrical since all nodes behave according to the same laws, the interactions should also be symmetrical. Interchanging two nodes should not change anything because the nodes should behave the same way when in the same situation.

Typically, F and G are nonlinear functions and for large systems the problem remains hard to solve. For large systems we can however introduce a mean field approximation.

2.1 A mean field Approximation

Here we repeat the steps proposed by Gao et al to obtain the mean field equation.

Assuming that the system can be described by some order parameter x_{eff} that reflects the behaviour of an effective (or average) node of the system. Gao et al. provide us with a mean field approximation that embodies a weighted average over all x_i's [1].

They propose a linear operator $\mathcal{L}$ that is defined in order to obtain x_{eff} is such that it takes the weighted average over a vector where the weight of a node is determined by the local coupling interaction with the rest of the system.

$$\mathcal{L}(\mathbf{w}) \equiv \frac{\mathbf{1}^T A \mathbf{w}}{\mathbf{1}^T A \mathbf{1}} \tag{2.3}$$

Here $\mathbf{1}$ is the vector of ones, effectively summing over the adjacency matrix A. Applying $\mathcal{L}$ to the vector $\mathbf{x}$ gives us the effective parameter that will have a central role throughout this work

$$x_{\text{eff}} \equiv \mathcal{L}(\mathbf{x}) = \frac{\mathbf{1}^T A \mathbf{x}}{\mathbf{1}^T A \mathbf{1}} \tag{2.4}$$

Using this in Eq. (2.2) gives us

$$\begin{aligned} \dot{x}_{\text{eff}} &= \frac{\sum_{i=1}^{N}\sum_{j=1}^{N} A_{ij}\dot{x_j}}{\sum_{i=1}^{N}\sum_{j=1}^{N} A_{ij}} \\ &\approx \frac{\sum_{i=1}^{N}\sum_{j=1}^{N} A_{ij} F(x_{\text{eff}})}{\sum_{i=1}^{N}\sum_{j=1}^{N} A_{ij}} + \frac{\sum_{i=1}^{N}\sum_{j=1}^{N} A_{ij}\sum_{k=1}^{N} A_{jk} G(x_{\text{eff}}, x_{\text{eff}})}{\sum_{i=1}^{N}\sum_{j=1}^{N} A_{ij}} \\ &= F(x_{\text{eff}}) + \beta_{\text{eff}} G(x_{\text{eff}}, x_{\text{eff}}) \end{aligned} \tag{2.5}$$

where the "effective" parameter β_{eff} describes the average coupling interaction strength in the system and is given by

$$\beta_{\text{eff}} = \frac{\sum_{i=1}^{N}\sum_{j=1}^{N} A_{ij} s_j^{\text{in}}}{\sum_{i=1}^{N}\sum_{j=1}^{N} A_{ij}} \tag{2.6}$$

Here s_j^{in} is the in degree of node j, with $s_j^{\text{in}} = \sum_{k=1}^{N} A_{jk}$.

At this point we should take a step back and note two key things. First, the assumption that the state and behavior of a network can be modeled by a single effective parameter is quite a stretch and limits the range of networks these assumptions are valid for. In general the assumptions are only valid for mutualisic networks [11], networks where all the interaction strengths between nodes are positive. We can make this intuitively acceptable by thinking of a competitive network of two nodes that will drive apart as time goes on, the effective node in this case will be the average of the two and thus stay somewhere in between the values of the competing nodes, not displaying what is going on in the system at all. We still remain with a broad class of networks that are definitely worth investigating.

Second, it should be noted that we got here by applying a linear operator $\mathcal{L}$ on x and A, or, if we want to be precise, rather applying it to $\dot{x}$. If we want to write our system in the form of Eq. (2.5) we have three options. The first option is that we only take into account systems in which F and G are linear in x_i as well as x_j, this however really limits the scope of the potential practical applications since these systems are most likely solvable analytically thus we don't need this method in the first place.

The second option we have is that we be content with this being an inequality, or rather, assuming

$$\mathcal{L}(F(x_i)) \approx F(\mathcal{L}(x_i)) = F(x_{\text{eff}}), \tag{2.7}$$

and

$$\mathcal{L}\Big(\sum_j A_{ij} G(\mathbf{x}, x_j)\Big) \approx \mathcal{L}\Big(\sum_j A_{ij}\Big) G(\mathcal{L}(\mathbf{x}), \mathcal{L}(\mathbf{x})) = \beta_{\text{eff}} G(x_{\text{eff}}, x_{\text{eff}}) \tag{2.8}$$

These approximations are numerically tested by Gao et al. for a range of networks but the validity of the assumptions has been questioned [11] and requires some mathematical justification.

Intuitively the idea of an order parameter defined as above makes a lot of sense. However, the mathematical derivation seems lacking. The main problems are a missing expression for the error made by assuming $\mathbf{x} = x_{\text{eff}}$ and the assumptions made in Eq. (2.7) and Eq. (2.8). Therefore we will explore the third option, a new derivation, in depth in the following chapter. First we will take a look at an example of a network to see why a mean field approximation could be useful int he first place.

2.2 An Example: Gene Regulatory Networks

We'll follow Gao et al. by looking at a gene regulatory network governed by the Michaelis-Menten equation [12]

$$\dot{x}_i = -B x_i^l + \sum_{j=1}^{N} A_{ij} \frac{x_j^h}{x_j^h + 1} \tag{2.9}$$

where the self-dynamics $F(x_i) = -B x_i^l$ describe degradation for $l = 1$ or dimerization for $l = 2$ and the coupling term $G(x_i, x_j) = x_j^h/(x_j^h + 1)$ embodies genetic activation. h is the Hill coefficient and captures the level of cooperation in the gene regulation.

We can immediately see that for a large amount of genes and a possibly complex coupling A the system of equations is hard to solve, even numerically. When in a stable equilibrium, it is also difficult to see which parameter changes will have which consequences. We'll take $B = l = h = 1$. If we now apply Gao's formalism we obtain the one dimensional effective equation that should solve the above problems.

$$\dot{x}_{\text{eff}} = -B x_{\text{eff}} + \beta_{\text{eff}} \frac{x_{\text{eff}}}{x_{\text{eff}} + 1} \tag{2.10}$$

where the assumption (2.7) is exact in this case, it is however not clear at all if (2.8) holds.

The new equation is claimed to describe the average behaviour of the system and reduces the topology of the system into the effective parameter β_{eff}. This equation is easily solved numerically and possibly even analytically, thereby allowing much more detailed analysis of the equilibria and the impact that the parameters have.

Chapter 3

Derivation of the Mean Field Equation and the Error

So far we have not convincingly derived Gao's mean field equations. Therefore here is a new attempt. We start from

$$\dot{x}_i = F(x_i) + \sum_{j=1}^{N} A_{ij} G(x_i, x_j) \tag{3.1}$$

We will make **2** assumptions (A1,A2) that should be satisfied in order to be able to validate the newly derived equation. The first assumption is:

A1. x_j in Eq. (3.1) can be replaced by $\sum_j A_{ij} x_j / \sum_k A_{ik}$. This physically amounts to a mean field assumption in the sense that the sum of interactions between node i and a number of nodes j is replaced by an average interaction.

If we rewrite Eq. (3.1) using assumption (A1) we obtain

$$\dot{x}_i = F(x_i) + s_i^{\text{in}} G\left(x_i, \sum_{j=1}^{N} A_{ij} x_j / \sum_{k=1}^{N} A_{ik} \right), \tag{3.2}$$

where the in-degree of node i, denoted as $s_i^{\text{in}} = \sum_{j=1}^{N} A_{ij}$ (note that the function G no longer depends on x_j which lets us take it outside of the sum).

Now we make the second approximation (A2):

A2. Another averaging procedure is performed. The local average over the x_j is approximately equal to the global average:

$$\frac{\sum_{j=1}^{N} A_{ij} x_j}{\sum_{j=1}^{N} A_{ij}} = \frac{\sum_{j,i=1}^{N} A_{ij} x_j}{\sum_{j,i=1}^{N} A_{ij}} - \delta_i$$

The δ_i determines how much the global average differs from the local average around node i and is assumed to be small, that is $\delta_i \to 0$ in some sense.

This immediately defines a quantity x_{eff}

$$x_{\text{eff}} \equiv \frac{\sum_{j,i=1}^{N} A_{ij} x_j}{\sum_{j,i=1}^{N} A_{ij}} \tag{3.3}$$

So after applying assumption (A2) we arrive at

$$\dot{x}_i = F(x_i) + s_i^{\text{in}} G\left(x_i, x_{\text{eff}} - \delta_i\right) \tag{3.4}$$

This non-linear differential equation (3.4) should be solved in the limit of $\delta_i \to 0$. From the expression for $x_i(t)$ in terms of (integrals containing) the unknown function $x_{\text{eff}}(t)$, we can next calculate x_{eff} using definition (3.3). The requirement of a self-consistent solution then leads to an equation for $x_{\text{eff}}(t)$, whose solution is equivalent to Gao's.

Let us illustrate how this works by considering the example of the gene network. In that case our equations read

$$\dot{x}_i = -B x_i + \sum_{j=1}^{N} A_{ij} \frac{x_j}{1 + x_j} \tag{3.5}$$

Applying the assumptions (A1,A2) to Eq. (3.5) results in equation

$$\dot{x}_i = -B x_i + s_i^{\text{in}} \frac{x_{\text{eff}} - \delta_i}{1 + x_{\text{eff}} - \delta_i} \tag{3.6}$$

We can solve these equations in the limit of $\delta_i \to 0$, which gives

$$x_i(t) = x_i(0) e^{-Bt} + s_i^{\text{in}} \int_0^t e^{-B(t-t')} \frac{x_{\text{eff}}(t')}{1 + x_{\text{eff}}(t')} \, dt' \tag{3.7}$$

Using now the definition for $x_{\text{eff}}(t)$ (Eq. 3.3) gives

$$x_{\text{eff}}(t) = \frac{\sum_{i,j} A_{ij} x_j(0) e^{-Bt} + \sum_{ij} A_{ij} s_j^{\text{in}} e^{-Bt} \int_0^t e^{Bt'} \frac{x_{\text{eff}}(t')}{1 + x_{\text{eff}}(t')} \, dt'}{\sum_{i,j} A_{ij}} \tag{3.8}$$

First multiplying by e^{Bt} and next differentiating gives exactly

$$\dot{x}_{\text{eff}} = -B x_{\text{eff}} + \beta_{\text{eff}} \frac{x_{\text{eff}}}{1 + x_{\text{eff}}}, \tag{3.9}$$

where $\beta_{\text{eff}} = \frac{\sum_{ij} A_{ij} s_j^{\text{in}}}{\sum_{ij} A_{ij}}$. If we solve Eq. (3.9) we know the dynamics of all nodes provided the assumptions imposed are valid.

This example works so well because the function $F(x)$ is linear in x. Let's now try this for more general functions. In this case it is no longer possible to directly find an expression for x_i in terms of $x_{\text{eff}}(t)$, so we need to deal with the differential equation itself. We can derive a differential equation for x_{eff}

from its definition

$$\begin{aligned}
\dot{x}_{\text{eff}} &= \frac{\sum_{i=1}^{N}\sum_{j=1}^{N} A_{ij}\dot{x}_j}{\sum_{i=1}^{N}\sum_{j=1}^{N} A_{ij}} \\
&\approx \frac{\sum_{i=1}^{N}\sum_{j=1}^{N} A_{ij}F(x_j)}{\sum_{i=1}^{N}\sum_{i=j}^{N} A_{ij}} + \frac{\sum_{i=1}^{N}\sum_{j=1}^{N} A_{ij}s_j^{\text{in}}G(x_j, x_{\text{eff}}-\delta_j)}{\sum_{i=1}^{N}\sum_{j=1}^{N} A_{ij}} \\
&\approx \frac{\sum_{i=1}^{N}\sum_{j=1}^{N} A_{ij}F(x_j)}{\sum_{i=1}^{N}\sum_{j=1}^{N} A_{ij}} + \frac{\sum_{i=1}^{N}\sum_{j=1}^{N} A_{ij}s_j^{\text{in}}G(x_j, x_{\text{eff}})}{\sum_{i=1}^{N}\sum_{j=1}^{N} A_{ij}} \\
&\quad - \frac{\sum_{i=1}^{N}\sum_{j=1}^{N} A_{ij}s_j^{\text{in}}\delta_j \frac{\partial G}{\partial x_2}(x_j, x_{\text{eff}})}{\sum_{i=1}^{N}\sum_{j=1}^{N} A_{ij}}
\end{aligned} \tag{3.10}$$

We'll now explore the three terms we've ended up with separately, first

$$\frac{\sum_{i=1}^{N}\sum_{j=1}^{N} A_{ij}F(x_j)}{\sum_{i=1}^{N}\sum_{j=1}^{N} A_{ij}} \tag{3.11}$$

where we should note that, since we are summing over terms of A_{ij}, any error we get when applying (A1) and (A2) and thus switching from x_j to x_{eff} should be interpreted as an error in the local average around node i. We end up with

$$\begin{aligned}
\frac{\sum_{i=1}^{N}\sum_{j=1}^{N} A_{ij}F(x_j)}{\sum_{i=1}^{N}\sum_{j=1}^{N} A_{ij}} &\approx \frac{\sum_{i=1}^{N} s_i^{\text{in}}F(x_{\text{eff}}-\delta_i)}{\sum_{i=1}^{N}\sum_{j=1}^{N} A_{ij}} \\
&\approx F(x_{\text{eff}}) - \frac{\sum_{i=1}^{N} s_i^{\text{in}}\delta_i}{\sum_{j=1}^{N}\sum_{i=1}^{N} A_{ij}}\frac{\partial F}{\partial x}(x_{\text{eff}})
\end{aligned} \tag{3.12}$$

Here we took a first order Taylor expansion, this holds as long as the errors δ are small enough. On to the next term, we start from

$$\frac{\sum_{i=1}^{N}\sum_{j=1}^{N} A_{ij}s_j^{\text{in}}G(x_j, x_{\text{eff}})}{\sum_{i=1}^{N}\sum_{j=1}^{N} A_{ij}} \tag{3.13}$$

Here we should again interpret these contributions as errors in the local average around node i, consequently resulting in the errors δ_i. Also using both (A1) and (A2) and a first order Taylor expansion nets us

$$\begin{aligned}
\frac{\sum_{i=1}^{N}\sum_{j=1}^{N} A_{ij}s_j^{\text{in}}G(x_j, x_{\text{eff}})}{\sum_{i=1}^{N}\sum_{j=1}^{N} A_{ij}} &\approx \frac{\sum_{i=1}^{N}\sum_{j=1}^{N} A_{ij}s_j^{\text{in}}G(x_{\text{eff}}-\delta_i, x_{\text{eff}})}{\sum_{i=1}^{N}\sum_{j=1}^{N} A_{ij}} \\
&\approx \frac{\sum_{i=1}^{N}\sum_{j=1}^{N} A_{ij}s_j^{\text{in}}}{\sum_{i=1}^{N}\sum_{j=1}^{N} A_{ij}}G(x_{\text{eff}}, x_{\text{eff}}) \\
&\quad - \frac{\sum_{i=1}^{N}\sum_{j=1}^{N} A_{ij}s_j^{\text{in}}\delta_i}{\sum_{i=1}^{N}\sum_{j=1}^{N} A_{ij}}\frac{\partial G}{\partial x_1}(x_{\text{eff}}, x_{\text{eff}}) \\
&= \beta_{\text{eff}}G(x_{\text{eff}}, x_{\text{eff}}) - \frac{\sum_{i=1}^{N}\sum_{j=1}^{N} A_{ij}s_j^{\text{in}}\delta_i}{\sum_{i=1}^{N}\sum_{j=1}^{N} A_{ij}}\frac{\partial G}{\partial x_1}(x_{\text{eff}}, x_{\text{eff}})
\end{aligned} \tag{3.14}$$

Which is where we will get our $\beta_{\text{eff}}G(x_{\text{eff}}, x_{\text{eff}})$ term from in the $\delta \to \mathbf{0}$ limit. Now the last term remains, we'll apply the same steps here to obtain

$$\begin{aligned}
\frac{\sum_{i=1}^{N}\sum_{j=1}^{N} A_{ij} s_j^{\text{in}} \delta_j \frac{\partial G}{\partial x_2}(x_j, x_{\text{eff}})}{\sum_{i=1}^{N}\sum_{j=1}^{N} A_{ij}} &\approx \frac{\sum_{i=1}^{N}\sum_{j=1}^{N} A_{ij} s_j^{\text{in}} \delta_j \frac{\partial G}{\partial x_2}(x_{\text{eff}} - \delta_i, x_{\text{eff}})}{\sum_{i=1}^{N}\sum_{j=1}^{N} A_{ij}} \\
&\approx \frac{\sum_{i=1}^{N}\sum_{j=1}^{N} A_{ij} s_j^{\text{in}} \delta_j}{\sum_{i=1}^{N}\sum_{j=1}^{N} A_{ij}} \frac{\partial G}{\partial x_2}(x_{\text{eff}}, x_{\text{eff}}) \\
&\quad - \frac{\sum_{i=1}^{N}\sum_{j=1}^{N} A_{ij} s_j^{\text{in}} \delta_j \delta_i}{\sum_{i=1}^{N}\sum_{j=1}^{N} A_{ij}} \frac{\partial^2 G}{\partial x_2 \partial x_1}(x_{\text{eff}}, x_{\text{eff}}) \qquad (3.15)
\end{aligned}$$

These three together result in a differential equation for x_{eff}

$$\begin{aligned}
\dot{x}_{\text{eff}} \approx\ & F(x_{\text{eff}}) + \beta_{\text{eff}} G(x_{\text{eff}}, x_{\text{eff}}) \\
& - \frac{\sum_{i=1}^{N} s_i^{\text{in}} \delta_i}{\sum_{j=1}^{N}\sum_{i=1}^{N} A_{ij}} \frac{\partial F}{\partial x}(x_{\text{eff}}) - \frac{\sum_{i=1}^{N}\sum_{j=1}^{N} A_{ij} s_j^{\text{in}} \delta_i}{\sum_{i=1}^{N}\sum_{j=1}^{N} A_{ij}} \frac{\partial G}{\partial x_1}(x_{\text{eff}}, x_{\text{eff}}) - \\
& \frac{\sum_{i=1}^{N}\sum_{j=1}^{N} A_{ij} s_j^{\text{in}} \delta_j}{\sum_{i=1}^{N}\sum_{j=1}^{N} A_{ij}} \frac{\partial G}{\partial x_2}(x_{\text{eff}}, x_{\text{eff}}) + \frac{\sum_{i=1}^{N}\sum_{j=1}^{N} A_{ij} s_j^{\text{in}} \delta_j \delta_i}{\sum_{i=1}^{N}\sum_{j=1}^{N} A_{ij}} \frac{\partial^2 G}{\partial x_2 \partial x_1}(x_{\text{eff}}, x_{\text{eff}}) \qquad (3.16)
\end{aligned}$$

Where for small δ we can drop the very last term as it is quadratic in δ whereas the rest of the terms (with δ in them) obey a linear dependence. If the terms involving $\delta_i \to 0$ as in assumption (A2) then we find again the Gao mean field equation. However, in the general case it is not clear that this will always be the case.

In order to find an expression for the errors δ we have to evaluate the right-hand side of the assumption in a similar fashion. Taking the same steps as before we end up with a slightly different expression, as expected

$$
\begin{aligned}
\frac{\sum_{j=1}^N A_{ij}\dot{x}_j}{\sum_{j=1}^N A_{ij}} &= \frac{\sum_{j=1}^N A_{ij}F(x_j)+\sum_{k=1}^N A_{jk}G(x_j,x_k)}{\sum_{j=1}^N A_{ij}} \\
&\approx F(x_{\mathsf{eff}}-\delta_i)+\frac{\sum_{j=1}^N A_{ij}s_j^{\mathrm{in}}G(x_j,x_{\mathsf{eff}}-\delta_i)}{\sum_{j=1}^N A_{ij}} \\
&\approx F(x_{\mathsf{eff}})-\delta_i\frac{\partial F}{\partial x}(x_{\mathsf{eff}}) \\
&\quad +\frac{\sum_{j=1}^N A_{ij}s_j^{\mathrm{in}}G(x_j,x_{\mathsf{eff}})}{\sum_{j=1}^N A_{ij}}-\frac{\sum_{j=1}^N A_{ij}s_j^{\mathrm{in}}\delta_j}{\sum_{j=1}^N A_{ij}}\frac{\partial G}{\partial x_2}(x_j,x_{\mathsf{eff}}) \\
&\approx F(x_{\mathsf{eff}})-\delta_i\frac{\partial F}{\partial x}(x_{\mathsf{eff}}) \\
&\quad +\frac{\sum_{j=1}^N A_{ij}s_j^{\mathrm{in}}G(x_{\mathsf{eff}}-\delta_i,x_{\mathsf{eff}})}{\sum_{j=1}^N A_{ij}}-\frac{\sum_{j=1}^N A_{ij}s_j^{\mathrm{in}}\delta_j}{\sum_{j=1}^N A_{ij}}\frac{\partial G}{\partial x_2}(x_{\mathsf{eff}}-\delta_i,x_{\mathsf{eff}}) \\
&\approx F(x_{\mathsf{eff}})-\delta_i\frac{\partial F}{\partial x}(x_{\mathsf{eff}}) \\
&\quad +\frac{\sum_{j=1}^N A_{ij}s_j^{\mathrm{in}}}{\sum_{j=1}^N A_{ij}}G(x_{\mathsf{eff}},x_{\mathsf{eff}})-\frac{\sum_{j=1}^N A_{ij}s_j^{\mathrm{in}}\delta_i}{\sum_{j=1}^N A_{ij}}\frac{\partial G}{\partial x_1}(x_{\mathsf{eff}},x_{\mathsf{eff}}) \\
&\quad -\frac{\sum_{j=1}^N A_{ij}s_j^{\mathrm{in}}\delta_j}{\sum_{j=1}^N A_{ij}}\frac{\partial G}{\partial x_2}(x_{\mathsf{eff}},x_{\mathsf{eff}})+\frac{\sum_{j=1}^N A_{ij}s_j^{\mathrm{in}}\delta_i\delta_j}{\sum_{j=1}^N A_{ij}}\frac{\partial^2 G}{\partial x_1\partial x_2}(x_{\mathsf{eff}},x_{\mathsf{eff}}) \qquad (3.17)
\end{aligned}
$$

where again, we could leave out the last term as it is quadratic in the error. After having done all this work we can now simply fill in the definition of δ_i and differentiate it with respect to time. We find

$$
\begin{aligned}
\dot{\delta}_i &= \frac{\partial F}{\partial x}(x_{\mathsf{eff}})\left[\delta_i-\frac{\sum_{j=1}^N s_i^{\mathrm{in}}\delta_i}{\sum_{i=1}^N\sum_{j=1}^N A_{ij}}\right]+G(x_{\mathsf{eff}},x_{\mathsf{eff}})\left[\beta_{\mathsf{eff}}-\frac{\sum_{j=1}^N A_{ij}s_j^{\mathrm{in}}}{\sum_{j=1}^N A_{ij}}\right] \\
&\quad +\frac{\partial G}{\partial x_1}(x_{\mathsf{eff}},x_{\mathsf{eff}})\left[\beta_{\mathsf{eff}}\delta_i-\frac{\sum_{i=1}^N\sum_{j=1}^N A_{ij}s_j^{\mathrm{in}}\delta_i}{\sum_{i=1}^N\sum_{j=1}^N A_{ij}}\right] \\
&\quad +\frac{\partial G}{\partial x_2}(x_{\mathsf{eff}},x_{\mathsf{eff}})\left[\frac{\sum_{j=1}^N A_{ij}s_j^{\mathrm{in}}\delta_j}{\sum_{j=1}^N A_{ij}}-\frac{\sum_{i=1}^N\sum_{j=1}^N A_{ij}s_j^{\mathrm{in}}\delta_j}{\sum_{i=1}^N\sum_{j=1}^N A_{ij}}\right] \qquad (3.18)
\end{aligned}
$$

where we have now dropped higher order terms in δ. Eqs. (3.16) and (3.18) together determine the evolution of x_{eff} and hence of x_i. We remark that the partial derivatives are to be evaluated at $x_{\mathsf{eff}}(t)$. The way to solve this system of equations is to suppose δ_j to be small, solve the mean field equation and next substitute the value obtained for x_{eff} in the equation (3.18) for δ_i and (numerically) integrate. If it turns out that δ stays small over time, the assumptions work well and the mean field approximation holds.

Chapter 4

Plants and Pollinators

An example of a mutualistic network is one that is an ecosystem that consists of plants an pollinators that contribute to each others abundance. This is also used as an example by Gao et al. Here x_i tracks the abundance of a plant species i:

$$\dot{x_i} = B_i + x_i\left(1 - \frac{x_i}{K_i}\right)\left(\frac{x_i}{C_i} - 1\right) + \sum_j A_{ij}\frac{x_i x_j}{D_i + E_i x_i + H_j x_j}, \tag{4.1}$$

where the first term resembles constant migration, the second describes logistic growth where the cubic growth model resembles the Allee effect. The Allee effect [13] correlates population size and mean individual fitness, population growth is skewed negatively for low population sizes. The effect can for example be witnessed in fish populations that have been over-fished, these populations might never recover from the damage that has been done to their species and thus live on in a low abundance state or go extinct. The third term resembles the interaction between plants j and i. The adjacency matrix A encompasses the strength of the interaction that plant j has on plant i. Note that the plants are not directly connected, they are part of a bipartite network of plants and pollinators in which the plants only have connections to pollinators and vice versa. To illustrate this, on the left is the bipartite network and on the right the resulting network.

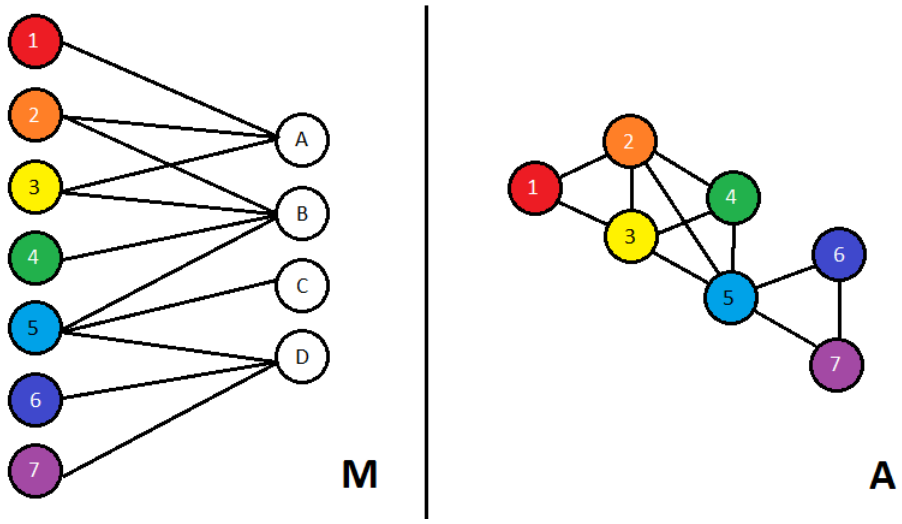

Figure 4.1: The bipartite network on the left, with corresponding matrix M. The resulting network is given on the right, with corresponding matrix A.

The interaction between two plants is stronger the more pollinators they share, but weaker the more plants the shared pollinators pollinate. The adjacency matrix is therefore constructed as

$$A_{ij} = \sum_{k=1}^{m} \frac{M_{ik} M_{jk}}{\sum_{s=1}^{n} M_{sk}}, \tag{4.2}$$

where M is a matrix with ones and zeroes that describes which pollinators pollinate which plants. To get an idea what kind of behaviour Eq. (4.1) resembles we'll show the relationship between the population growth of a species and it's population size for some common values for the parameters and a fixed environment

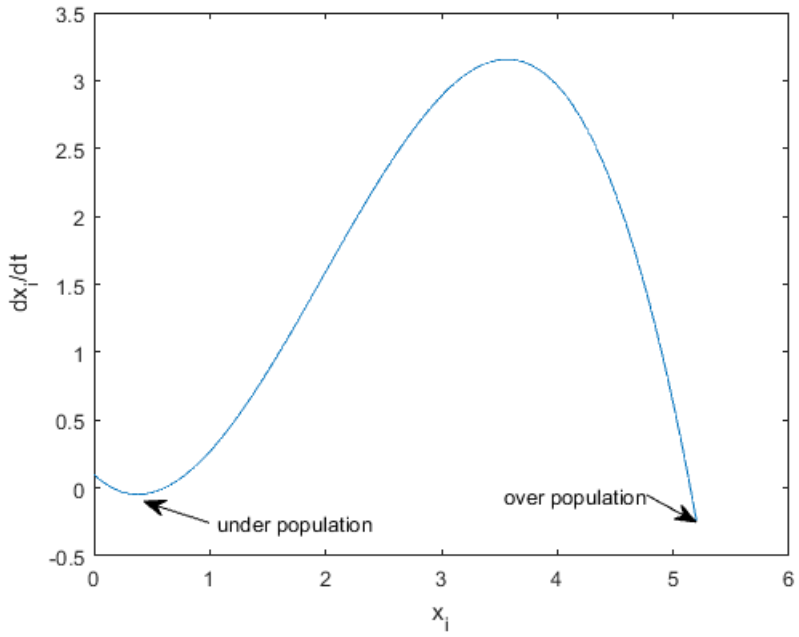

Figure 4.2: The abundance growth of a plant depicted versus its abundance. For low population sizes we can clearly see the Allee effect take place, resulting in negative growth. For larger abundances the growth grows accordingly. If the abundance becomes too large we see some over population effect take place so that the growth decays very quickly and turns negative. The values of the parameters are: $B = 0.1$,$K = 5$,$C = 1$,$D = 5$,$E = 0.9$,$H = 0.1$ [1], these values will be used throughout this study.

Applying the mean field approximation gives us the following 1D effective differential equation for the effective abundance of the plants

$$\dot{x}_{\text{eff}} = B + x_{\text{eff}}\left(1 - \frac{x_{\text{eff}}}{K}\right)\left(\frac{x_{\text{eff}}}{C} - 1\right) + \beta_{\text{eff}}\frac{x_{\text{eff}}^2}{D + (E+H)x_{\text{eff}}} \tag{4.3}$$

At this point we should throw in a bifurcation diagram. A bifurcation diagram shows us where the fixed points of the network lie and how this changes with parameter values. In this case we are interested to see where the fixed points of the effective equation lie as a function of the effective parameter β_{eff}. This lets us understand in which regions the dynamics of the network behave in what way. The resilience of a network is its resistance against perturbations, its capability to return to its original state after being perturbed. When a system is in a stable equilibrium, it will correct for small perturbations acting upon it. If, however, the system is heavily disturbed, this change can force the system to go to another stable equilibrium.

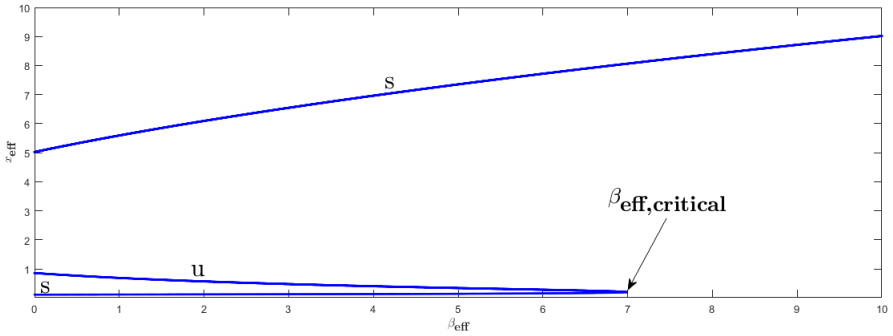

Figure 4.3: The bifurcation diagram for the effective equation where the order parameter x_{eff} is plotted versus the effective parameter β_{eff}. The upper and lower curves represent stable equilibria of the effective system. The branch in between is an unstable equilibrium. The point indicated with $\beta_{\text{eff,critical}}$ marks the value for β_{eff} from where only one stationary solution exists for the effective equation. We only show the physically relevant area where $x_{\text{eff}}, \beta_{\text{eff}} \geq 0$.

When we find the system in its low abundance stable steady state, a perturbation can force it over the unstable steady state. The system will from there move toward the high abundance stable state. From there it is much harder for a perturbation to go back to the low abundance stable state since the perturbation will have to force the system all the way back over the unstable equilibrium, which is much further away from the high abundance, stable state. We should also note that for large values of β_{eff} the effective system no longer has three equilibrium points, it only has one high abundance stable steady state. The effective system will for large β_{eff} always converge to this state if given enough time.

Following up on this, it would be interesting to see how this critical value of the effective parameter depends on the size of the network it is trying to describe. What happens to the network and its mean field approximation when the link strength between nodes is perturbed by some external influence? We can simulate this perturbation by introducing a parameter $p \in (0, 1)$ and scale A linearly with p, that is $\tilde{A} = pA$. The resilience of the network is its ability to withstand the perturbation, it is determined by the effective parameter β_{eff}. This means that the critical value for p, the one where the network will remain in a low abundance state when it starts there, scales as

$$\beta_{\text{eff}} = \frac{\mathbf{1}\tilde{A}^2\mathbf{1}}{\mathbf{1}\tilde{A}\mathbf{1}} \sim \frac{(pN)^2}{pN} = pN \tag{4.4}$$

$$p_{\text{crit}} \sim \frac{\beta_{\text{eff,crit}}}{N} \tag{4.5}$$

This result can be viewed in the figure below as well. We performed numerical simulations in MATLAB, giving us a value for the critical point of the effective parameter as $\beta_{\text{eff,crit}} = 6.9 \pm 0.1$. When using a low initial condition, this is the turning point of β for which the system either goes to one or the other stable state instead of always going to the high abundance state (for large β_{eff}).

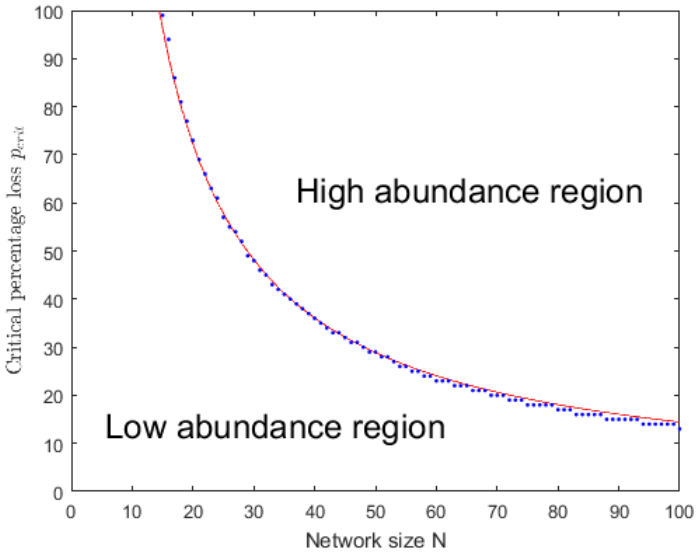

Figure 4.4: In blue are the critical values of p that we found with numerical, fitted against in red, the curve c/N where c is just a constant. After all, we only have a proportional relationship between p_{crit} and N. The network size versus the critical perturbation at which the system collapses to a low abundance state.

The figure shows an inverse proportionality between the network size N and the perturbation at which the system can only go to a high abundance state, indicating that Eq. (4.5) is indeed correct. The fact that the critical perturbation strength is dependant on the size of the network is an important observation. This implies that for large values of the effective parameter β_{eff} we should expect a less significant influence from perturbations such as noise that effects the system. These stochastic contributions will be discussed in the following chapter.

Chapter 5

Stochastic Perturbations

Many systems in reality are constantly perturbed by a wide range of effects such as thermal fluctuations in physics, a small change in global temperature or sudden rain in ecological systems or even the infamous Mondays for human behaviour. It is therefore important to see what happens to the resilience of the system and the resilience of the mean field approximation (and importantly, the difference between the two) when small perturbations act upon the system. These small changes of circumstances are often modelled as a stochastic variable as they are extremely hard to predict. We want to know what happens mathematically when we add a noise term to the equation. We will look at what happens when we add zero mean Gaussian noise to the self dynamics of each node i whose behavior will be described as

$$\dot{x_i} = B_i + x_i\left(1 - \frac{x_i}{K_i}\right)\left(\frac{x_i}{C_i} - 1\right) + \sum_j A_{ij}\frac{x_i x_j}{D_i + E_i x_i + H_j x_j} + \zeta_i \tag{5.1}$$

with ζ_i the perturbation in the behaviour of node i. We can imagine that for small variances in the noise not so much will change. However, if the perturbation of the noise is so high that x_i can use it to cross over to another stable solution, it might stay there indefinitely. As for the effective parameter, we are obliged to carry out our old recipe and apply our linear operator $\mathcal{L}$ on ζ to obtain some 'effective disturbance' in the system.

We know that $\zeta_i \sim N(0, \sigma^2)$ so we can say something about ζ_{eff}. Note that ζ_{eff} is the weighted sum of normally distributed variables with zero mean and variance σ^2. The average of these variables still has zero mean. The variance of the average of normally distributed variables is σ^2/N. So, as expected, for large systems the effective disturbance ζ_{eff} will have next to no influence on the system as a whole if the system is in a stable state, after all, if a system is in one of its stable states the stability requires the system to recover from small perturbations. If, however, a system is not in a stable state, a small perturbation can make the difference from going to one stable state instead of another. When this one node goes to lets say a high state, it can drag the others there as well (due to the mutualistic nature of the network), making the entire network go to a state it wouldn't have gone to without the perturbation present.

Let us look at an example of this behavior. First we should remember that a system will go to a high abundance state if the effective parameter β_{eff} is higher than it's critical value of around 6.9. Therefore, if we construct a network that has $\beta_{\text{eff}} \approx 6.9$, the perturbations could really make a difference. We have constructed such a network with 15 nodes and a chance of $\frac{1}{3}$ of a plant connecting to a pollinator. We found a network that has $\beta_{\text{eff}} = 5.1$ and solved Eq. (5.1) numerically with the Euler Forward method in MATLAB. The initial state that the network was brought into was a low abundance state. The noise applied was such that $\zeta_i \sim N(0, 25)$.

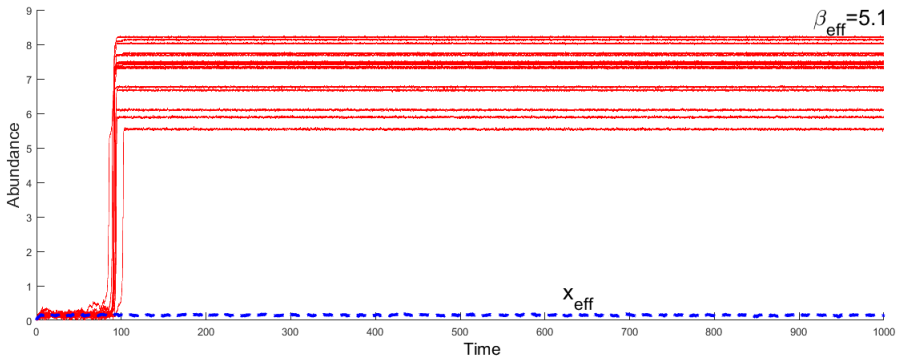

Figure 5.1: A network where the perturbation has a deciding influence on the behavior of the network. The blue, dashed line is the approximated behaviour obtained after applying the linear operator. The red lines are the actual nodes' abundances.

As we can see, the value of β_{eff} isn't enough to get x_{eff} to the high abundance state, but combined with the perturbation, it is enough to make first one, and then all x_i make the climb. Since the perturbation of x_{eff} is much smaller, it doesn't have enough influence on the behavior of x_{eff} in order to keep approximating the system properly.

If we make similar networks where β_{eff} is not close to it's critical value however, the approximation works way better.

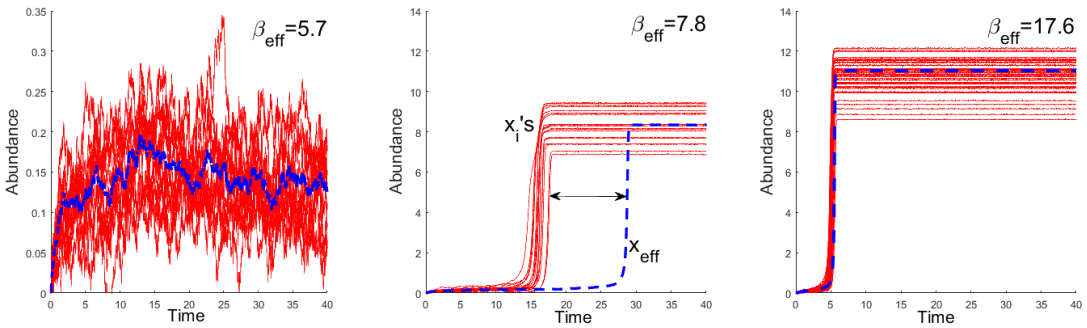

Figure 5.2: The blue, dashed line is the approximated value after applying the linear operator $\mathcal{L}$. The red lines are all of the actual nodes' abundances. a) The approximated x_{eff} remains in a low state of abundance, just like the actual abundances of the nodes. Note that the vertical scale indicates low values at all times. b) For this higher value of β_{eff}, the system goes into a high state of abundance as predicted by the approximation. It does take longer for x_{eff} to reach the high abundance state however, this is indicated by the double arrow. c) For even bigger β_{eff}, x_{eff} goes to the high abundance state just as fast as the actual nodes, the approximation excels here.

In the middle figure we can witness a remarkable phenomenon. The time it takes for the effective x to go to the high abundance state is much larger than for the actual nodes. A guess to why this happens is that the perturbation in x_{eff} is the weighted average over perturbations, thus having not as much influence as the noise that applies to the actual nodes of the system itself. The noise firsts "pushes" one of the nodes closer to the high abundance state. This node then works as a catalyst for the other nodes to go to their high abundance states. The mean field equation does not correctly encompass these mutual dynamics when noise is applied. In the other cases the approximation seems to hold just fine. As figure 5.1 indicates, there are situations where the combination of noise and connectedness of

the network result in failure of the approximation. When does this failure occur? And when does the approximation display the behaviour as witnessed in 5.2b? We will next inspect for which combinations of noise amplitude and network size these phenomena occur.

Using a network of 15 nodes, let us vary the amplitude of the noise and the value of β_{eff}. We know that for large values of β_{eff} the method does find the correct solution so we tried a range from 2 to 9, the entire adjacency matrix was scaled to obtain these values. The amplitude of the noise was ranged from 0.005 to 0.200. We let the system make 150 time steps using the Euler forward method. Since the noise is a stochastic process, an average was taken over 50 trials.

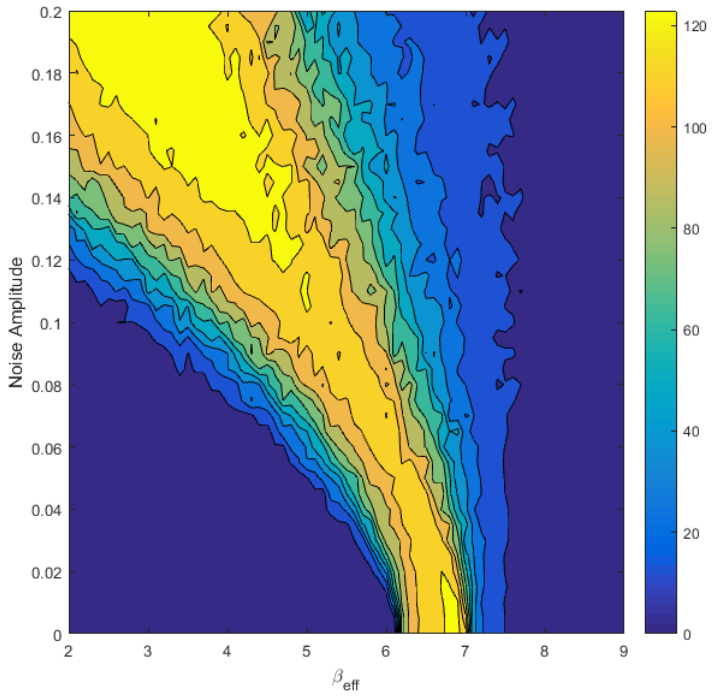

Figure 5.3: The color indicates how many time steps, on average, it took x_{eff} longer than the average of the abundances of the nodes, to go to the high abundance state. In other words, the more yellow, the longer it took for the method to converge to the actual value that is being approximated. In the right blue region we have a resemblance of the most right figure in 5.2, x_{eff} converges to the high abundance state at the same time as the actual nodes do so. In the left blue region we have a depiction of what we saw in the most left figure in 5.2, x_{eff} and the actual nodes both stay in the low abundance state. The middle, the yellow "ridge" resembles an area where the actual nodes do go to the high abundance state, but x_{eff} does not. On the left side of the yellow region we see that x_{eff} stays in the low abundance state while the actual nodes do go to the high abundance state some of the time. On the right of the yellow region we see that the time it takes for x_{eff} to catch up to the actual nodes and go to the high abundance state becomes less and less as β_{eff} increases. The total run time is 150 time steps and it takes some small amount of time steps before the actual nodes converge to the high abundance state. Since the most yellow region corresponds to a time difference of about 120 steps, we can conclude that the approximation does not converge to the correct value at all. It may be the case that this is due to a cut-off time. For large noise amplitudes and low values for β_{eff} we see that the actual nodes' abundances go to the high abundance state quickly, but x_{eff} stays in the low abundance state forever. As β_{eff} increases, x_{eff} also "benefits" from the noise in that it goes to the high abundance state even if it wouldn't have done so in the case of no noise.

Only if the entire graph were blue, indicating that there is no time difference between the real network

going to the high abundance state and the mean field approximation going to the high abundance state, we could conclude that the two are both influenced in the same way by stochastic perturbations. This is however not the case. From the middle part of the graph we can even conclude that in some situations, when $\beta_{\text{eff}} \approx \beta_{\text{eff,crit}}$, the mean field approximation does not approximate the real network at all. The two converge to two different values. The mean field approximation in this case stays in the low abundance state, whereas the the network is perturbed enough to go to the high abundance state. To better understand this behaviour we will have a closer look at the equilibria in the next chapter.

Chapter 6

Equilibria Investigated

To examine the method some further, we are going to look at the different steady state situations the model can find itself in. If we wait for the model to go to one of the steady state situations every time we run it (and this is indeed what we do), we should investigate whether the only stable solutions are in phase solutions (defined by $x_1 = x_2 = ... = x_N$), which is basically what is assumed by Gao et al. when we look at the effective equation for x_{eff}.

To find all time independent solutions we have to compute all **x** for which

$$\dot{\mathbf{x}} = \mathbf{0}. \tag{6.1}$$

This means that we should find zeroes of

$$0 = B_i + x_i\left(1 - \frac{x_i}{K_i}\right)\left(\frac{x_i}{C_i} - 1\right) + \sum_j A_{ij}\frac{x_i x_j}{D_i + E_i x_i + H_j x_j}, \text{for } i = 1, 2, ..., N \tag{6.2}$$

Finding exact solutions to this equation will be next to impossible for $N > 2$ since no closed form solutions exist for polynomials of order 5 or more. We must therefore resort to a numerical approach. The space in which these solutions live has a dimension equal to N, so determining zeroes becomes computationally harder rapidly for many-node-systems. Note that all the equations are coupled, so we cant solve them separately and we are stuck with the multidimensional problem. For 2, 3 and 4 dimensions we can still find all the solutions to these equations within acceptable computation time. For simplicity (and to keep some symmetry in the problem) we took $A_{ij} = 1$ for all i, j, so $\beta_{\text{eff}} = N - 1$. For the two dimensional case we find the following zeros using MATLABS's built in "fsolve" function, that uses a trust-region-dogleg algorithm by default, on a N dimensional grid that is finer spaced than the zeros that it found

Table 6.1: All of the steady state solutions of the two dimensional problem with stability qualifications for each point. The synchronization manifold contains two stable solutions and one unstable solution, the other solutions are saddle points. The two saddle points in this case are mirrored in the line $x_1 = x_2$.

x_1	x_2	Qualification
0.1196	0.1196	Stable
0.1500	0.8234	Saddle
0.8234	0.1500	
0.6912	0.6912	Unstable
5.5941	5.5941	Stable

In the three dimensional case we find some more zeros than we do in the two dimensional case. They are listed below

Table 6.2: All of the steady state solutions for the three dimensional case. Again we find that two stable solutions and one unstable solution lie on the line $x_1 = x_2 = x_3$, all the other solutions are saddle points.

x_1	x_2	x_3	Qualification
0.1241	0.1241	0.1241	Stable
0.7834	0.1573	0.1573	Saddle
0.1573	0.7834	0.1573	
0.1573	0.1573	0.7834	
0.5709	0.5709	0.5709	Unstable
0.1878	0.6524	0.6524	Saddle
0.6524	0.1878	0.6524	
0.6524	0.6524	0.1878	
6.0944	6.0944	6.0944	Stable

For the case of $N = 4$ we see that this trend continues:

Table 6.3: All of the steady state solutions for the four dimensional case. Once more we find that the solutions on the synchronization manifold are either stable or unstable, the two furthest apart being the stable solutions and the one in between the unstable one. Again, all other solutions are saddle points, this time in four dimensional space.

x_1	x_2	x_3	x_4	Qualification
0.1295	0.1295	0.1295	0.1295	Stable
0.7377	0.1667	0.1667	0.1667	Saddle
0.1667	0.7377	0.1667	0.1667	
0.1667	0.1667	0.7377	0.1667	
0.1667	0.1667	0.1667	0.7377	
0.4790	0.4790	0.4790	0.4790	Unstable
0.2314	0.5276	0.5276	0.5276	Saddle
0.5276	0.2314	0.5276	0.5276	
0.5276	0.5276	0.2314	0.5276	
0.5276	0.5276	0.5276	0.2314	
0.6068	0.6068	0.2017	0.2017	Saddle
0.6068	0.2017	0.6068	0.2017	
0.2017	0.6068	0.6068	0.2017	
0.6068	0.2017	0.2017	0.6068	
0.2017	0.6068	0.2017	0.6068	
0.2017	0.2017	0.6068	0.6068	
6.5470	6.5470	6.5470	6.5470	Stable

We will look some deeper into the two dimensional case for now, as this provides insight while it is still easy to display in this two dimensional paper. Next up we should see what these saddle points look like. In what direction are they attractive and in what direction are they repulsive? When do solutions end up in the low abundance stable solution, and when in the high abundance one? Below, two phase plots are displayed The figures show us the synchronization manifold of the system of equations. Synchronization is a very important topic in systems governed by coupled differential equations and is widely used to describe e.g. coupled oscillators, which we will encounter later on. The synchronization manifold is simply put the region in phase space where synchronization ($\dot{x}_1 = ... = \dot{x}_N$) occurs. The fixed points of a system must by definition lie on the synchronization manifold (since $\dot{x}_1 = ... = \dot{x}_N = 0$), which

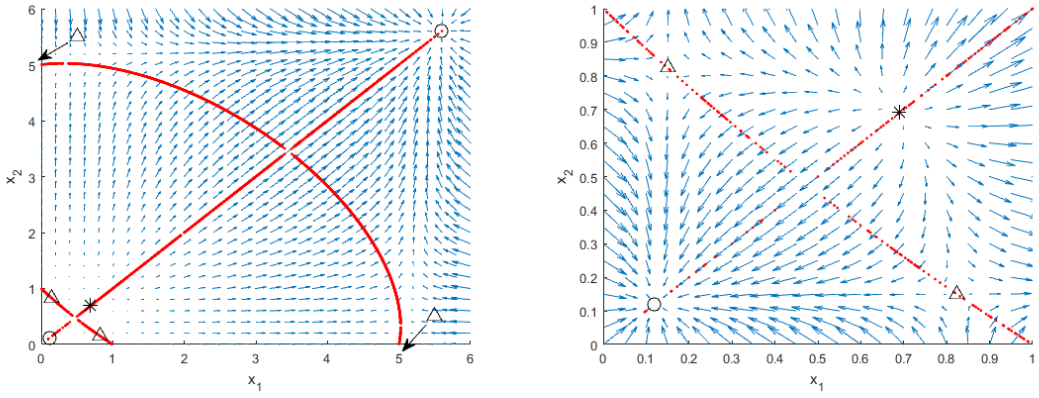

Figure 6.1: Here we see the phase plot in two dimensions. In each case the derivatives have been plotted as a vector $(\dot{x}_1, \dot{x}_2)$ as functions of the specific point in this 2D space. Since it is hard to see what is going on for small x the right figure zooms in on the lower left area of the left graph. The zeroes listed in table 6.1 are marked. The circles represent the stable fixed points, the star represents the unstable fixed point and the triangles represent saddle points. We can see that the zeros in the table are classified correctly by looking at the behaviour around the markers. We also see some strange behavior around the points $(5, 0)$ and $(0, 5)$. This is due to non-physical zeros (ones that are not within the first quadrant), saddle points, that lie close to the axes. The red points are points on the synchronization manifold. This is the set of points where $\dot{x}_1 = \dot{x}_2$.

we see happens in the figures above. We see, as suspected, in 4.3 that for small enough β_{eff} we find three fixed points on the line $x_1 = x_2 = x_{\text{eff}}$. Two of these are stable fixed points, they are also the only stable fixed points of the system. The saddle points that lie outside of the first quadrant are of no interest to us, they are non-physical solutions since no negative population sizes exist and with physical initial conditions the system will never go to one of those fixed points. Two more fixed points are found in the form of saddle points. There is only a closed set of points for the initial condition so that the system converges to these saddle points. In this two dimensional, symmetrical case, the phase plot and the synchronization manifold help us understand that the mean field approximation works in these scenarios and correctly finds in-phase solutions.

Chapter 7

Generalized Lotka-Volterra systems

In [11] it was argued that the method of an average abundance based solely on an average parameter does not work for Lotka-Volterra systems. It was also argued[10] that in some cases the method does not work for the General Lotka-Volterra model. To understand these claims in terms of the dynamical systems approach we investigate the ordinairy Lotka-Volterra, and the Generalized Lotka-Volterra systems in this section, starting with the oridnary Lotka-Volterra model.

This, as before, only encompasses the two dimensional case, where x_1 represents a prey population and x_2 describes a predator population. The Lotka-Volterra equations model these populations with the following equations

$$\dot{x_1} = \alpha x_1 - \beta x_1 x_2, \tag{7.1}$$

$$\dot{x_2} = \delta x_1 x_2 - \gamma x_2, \tag{7.2}$$

where α,β,γ,δ are all real, positive integers describing the interaction between the two species. We can solve the fixed points exactly, resulting in the points $(0,0), (\frac{\gamma}{\delta}, \frac{\alpha}{\beta})$. Here the origin of course corresponds to a zero-abundance state, or extinction. The stability of these points requires us to work with the Jacobian matrix, given as

$$J(x_1, x_2) = \begin{bmatrix} \alpha - \beta x_2 & \delta x_2 \\ -\beta x_1 & \delta x_1 - \gamma \end{bmatrix}$$

Computing stability of the two zeros by entering them into the Jacobian gives:

$$J(0,0) = \begin{bmatrix} \alpha & 0 \\ 0 & -\gamma \end{bmatrix}$$

with eigenvalues α and $-\gamma$. Since the parameters are all real and positive we can conclude the origin to be a saddle point. The eigenvector belonging to the eigenvalue α is $\hat{x_1}$ and the eigenvector belonging to the eigenvalue $-\gamma$ is $\hat{x_2}$, so the origin is repulsive toward the x_1 axis and attractive toward the x_2 axis. The other fixed point

$$J(\frac{\gamma}{\delta}, \frac{\alpha}{\beta}) = \begin{bmatrix} 0 & \frac{\delta\alpha}{\beta} \\ -\frac{\beta\gamma}{\delta} & 0 \end{bmatrix}$$

with eigenvalues $\pm i\sqrt{\alpha\gamma}$. These eigenvalues are purely imaginary, thus we can conclude the fixed point to be elliptic. Now we can finally understand why the method of Gao et al. is no good when analyzing this system. The assumption of being on the synchronization manifold is a dubious one in this case and does not describe the system whatsoever.

We next turn to the Generalised Lotka-Volterra dynamics, where the traditional equations are rewritten such that they are in the form of Eq. (2.2). The equations read

$$\dot{x_i} = \alpha x_i + x_i \sum_j A_{ij} x_j. \tag{7.3}$$

So that we can write $F(x) = \alpha x$ and $G(x_i, x_j) = x_i x_j$. As stated by Tu et al. the analytic solution for the stationary state $\mathbf{x} = -A^{-1}\alpha$ is easily obtained if A is invertible. It is however not clear if the system has stable solutions.

By applying Barabasi's formalism we find the one dimensional effective equation

$$\dot{x}_{\text{eff}} = \alpha x_{\text{eff}} + \beta x_{\text{eff}}^2, \tag{7.4}$$

where the stationary point $x_{\text{eff}} = -\frac{\alpha}{\beta}$ is stable with eigenvalue $-\alpha$. The point $x_{\text{eff}} = 0$ is also a fixed point of the system with eigenvalue α and is therefore unstable.

The fact that for any value of β_{eff} and thus for any adjacency matrix A we can find a stable fixed point for the 1D effective equation is worrying, as pointed out by Tu et al. There may very well be combinations of matrix entries for which the system has no stable stationary solutions. In those cases, Gao et al's framework gives a flat out wrong indication of the resilience of the network. Otherwise, the formalism will correctly predict stable solutions.

Chapter 8

The Kuramoto Model and Synchronization

The Kuramoto model describes a system of N coupled phase oscillators. The change of phase of oscillator v_i is described by[14]

$$\dot{\theta}_i = \omega_i + \frac{\kappa}{N}\sum_{j=1}^{N}\sin(\theta_j - \theta_i) \tag{8.1}$$

where each oscillator has its own natural frequency ω_i distributed with some probability density function $g(\omega)$ which is assumed to be normalized, is coupled to the other oscillators with some coupling constant κ and the coupling strength is normalized. In this case the function $F_i \neq F$, it is different for each oscillator. The coupling function G takes the form of a sine. This form of the Kuramoto model can be solved exactly in the $N \to \infty$ limit by using a mean field transformation of the form

$$re^{i\psi} = \frac{1}{N}\sum_{j=1}^{N} e^{i\theta_j}, \tag{8.2}$$

where r and ψ are order parameters, r represents the phase-coherence of the oscillators and ψ represents the average phase. Substituting this into Eq. (8.1) gives us the equation

$$\dot{\theta}_i = \omega_i + \kappa r\sin(\psi - \theta_i). \tag{8.3}$$

This equation is no longer directly coupled to the other oscillators' equations. Furthermore, when spacial topology allows for it, a rotating frame of reference is usually taken so that $\psi = 0$. In that case, the equation reduces to

$$\dot{\theta}_i = \omega_i - \kappa r\sin(\theta_i). \tag{8.4}$$

Let us continue to write Eq. (8.2) in another way:

$$re^{i\psi} = \int_{-\pi}^{\pi} e^{i\theta}\left(\frac{1}{N}\sum_{j=1}^{N}\delta(\theta - \theta_j)\right)\mathrm{d}x \tag{8.5}$$

For the limit where N goes to infinity we may assume that the oscillators are distributed according to a probability density function $\rho(\theta, \omega, t)$ given some ω which is on its own turn distributed by $g(\omega)$, as mentioned above. The mean in Eq. (8.2) is now replaced by an average over phase and frequency

$$re^{i\psi} = \int_{-\pi}^{\pi}\int_{-\infty}^{\infty} e^{i\theta}\rho(\theta, \omega, t)g(\omega)\mathrm{d}\omega\mathrm{d}\theta. \tag{8.6}$$

We'll have to assume the function $\rho(\theta, \omega, t)$ to be normalized, resulting in

$$\int_{-\pi}^{\pi} \rho(\theta, \omega, t) \mathrm{d}\theta = 1. \tag{8.7}$$

Next we should introduce a very handy relationship, the continuity equation. Noting that the angular or drift velocity of the oscillators is $v_i = w_i + \kappa r \sin(\psi - \theta_i)$ we find

$$\frac{\partial \rho}{\partial t} + \frac{\partial}{\partial \theta}\Big[\big(\omega + \kappa r \sin(\psi - \theta)\big)\rho(\theta, \omega, t)\Big] = 0 \tag{8.8}$$

where the right-hand side equals zero because there can be no production or dissipation of oscillators. Let us first consider some limit cases. A trivial solution is quickly found by setting $\rho = 1/2\pi$, there we find $r = 0$, corresponding to an incoherence state. All the oscillators run around freely and no synchronization occurs whatsoever. In the strong coupling limit, where κ goes to infinity, we expect all oscillators to have the same phase $\theta_i = \psi$. The density is concentrated in one place, so we find

$$re^{i\psi} = \int_{-\pi}^{\pi} e^{i\theta}\delta(\psi - \theta) \int_{-\infty}^{\infty} g(\omega)\mathrm{d}\omega\mathrm{d}\theta = \int_{-\pi}^{\pi} e^{i\theta}\delta(\psi - \theta)\mathrm{d}\theta = e^{i\psi}, \tag{8.9}$$

giving our order parameter as $r = 1$, global synchronization, or a total coherence state. Most interesting is perhaps the middle ground. The system where we have some finite r where some of the oscillators are locked and some roam without ever being caught in synchronization. An oscillator with drift (or angular) velocity $v = \omega + \kappa r \sin(\psi - \theta)$ will be locked if $\omega = \kappa r \sin(\theta - \psi)$. For oscillators with $|\omega| > \kappa r$ the natural frequency of the oscillator is too large for the oscillator to be locked in, here we can use the continuity equation to obtain the steady state result

$$\rho(\theta, \omega, t) = \frac{C}{\omega + \kappa r \sin(\psi - \theta)}, \tag{8.10}$$

where C is the integration constant and can be found later with the use of the normalization condition. For oscillators with a natural frequency $|\omega| < \kappa r$ the oscillators will be locked in at an angle $\theta - \psi - \sin^{-1}(\frac{w}{\kappa r})$. This locking is only stable if $-\pi/2 \leq \theta - \psi \leq \pi/2$ so we obtain a stable steady state of

$$\rho(\theta, \omega, t) = \begin{cases} \delta(\theta - \psi - \sin^{-1}(\frac{w}{\kappa r}))H(\cos(\theta)) & \text{if } |\omega| < \kappa r \\ \frac{C}{\omega + \kappa r \sin(\psi - \theta)} & \text{else.} \end{cases} \tag{8.11}$$

Calculating C with the use of Eq. (8.7) results in $C = \frac{\sqrt{\omega^2 - \kappa^2 r^2}}{2\pi}$. From this we can express our order parameter in terms of Eq. (8.11)

$$re^{i\psi} = \int_{-\pi/2}^{\pi/2} \int_{-\infty}^{\infty} \delta(\theta - \psi - \sin^{-1}(\frac{\omega}{\kappa r}))g(\omega)\mathrm{d}\omega\mathrm{d}\theta + \int_{-\pi}^{\pi} \int_{|\omega| > \kappa r} \frac{Cg(\omega)}{\omega + \kappa r \sin(\psi - \theta)}\mathrm{d}\omega\mathrm{d}\theta. \tag{8.12}$$

At this point we're going to have to assume a density $g(\omega)$ if we would want to continue our analysis.

8.1 Connection to Gao et al.'s work

What happens if we try to describe this model in terms of an effective parameter the way that Gao et al. do? First we'll do a naive approach to see what happens. Lets call our effective parameter θ_{eff} and use that $\mathcal{L}(G(\theta)) \approx G(\theta_{\text{eff}})$ we should note that the function $G(\theta_{\text{eff}}, \theta_{\text{eff}}) = 0$ for all values of θ_{eff}. This means that the effective parameter θ_{eff} in this case is never influenced by the coupling constant κ. The system it tries to describe is however greatly influenced by this constant as it determines to what length the system will be in a coherent or incoherent state. If we use a rotating frame of reference at

a radial frequency of ω_{eff}, Eq. (8.1) does not provide us with any information about the system. If we however do not claim that the sine function is linear and we use a tailor expansion we get

$$\mathcal{L}(\sin(\theta_j - \theta_i)) = \big(\mathcal{L}(\theta_i) - \mathcal{L}(\theta_j)\big) - \frac{\mathcal{L}\big((\theta_i - \theta_j)^3\big)}{3!} + \mathcal{L}(h.o.t.) \tag{8.13}$$

$$= \frac{1}{3!}\Big(\mathcal{L}(\theta_j^3) - 3\mathcal{L}(\theta_j^2\theta_i) + 3\mathcal{L}(\theta_j\theta_i^2) - \mathcal{L}(\theta_i^3)\Big) + \mathcal{L}(h.o.t.), \tag{8.14}$$

the linear term vanishes as discussed above. If we were to introduce another operator, one we could apply to higher order polynomials we still have a problem here. The symmetry of these uneven powers that the sine function gives us is such that any operator that works the same for θ_i as it does for θ_j always yields us no coupling contribution as all terms cancel by symmetry after the operator is applied to both phases. This method of approximation is inherently useless in the Kuramoto model stated above.

Let us now consider a different approach to the problem. We'll work with the order parameter r as Kuramoto defines in Eq. (8.2) and use our only degree of freedom to set $\psi = 0$. From now on we will use j for our subscripts by default as i will be the imaginary unit. We next introduce the variable $x_j(t)$ as

$$x_j = e^{i\theta_j} \tag{8.15}$$

for all j, so that

$$r = \frac{\sum_{j=1}^{N} 1 \cdot x_j}{\sum_{j=1}^{N} 1} = x_{\text{eff}} \tag{8.16}$$

is in the form of Gao's effective parameter. The differential equations for the x_j's are

$$\frac{dx_j(t)}{dt} = \frac{d(e^{i\theta_i})}{dt} = ie^{i\theta_j}\frac{d\theta_j}{dt} \tag{8.17}$$

$$= ix_j\big(\omega_j - Kr\sin(\theta_j)\big) \tag{8.18}$$

$$= i\omega_j x_j - \frac{Kr}{2}\big(e^{2i\theta_j} - 1\big) \tag{8.19}$$

$$= i\omega_j x_j + \frac{K}{2}(1 - x_j^2)r \tag{8.20}$$

$$= i\omega_j x_j + \sum_{l=1}^{N}\frac{K}{2N}(1 - x_j^2)x_l \tag{8.21}$$

$$= F_j(x_j) + \sum_{l=1}^{N} A_{j,l}G(x_j, x_l). \tag{8.22}$$

Where $F_j(x_j) = i\omega_j x_j$, $A_{j,l} = 1/N$ for $j \neq l$ and $G(x_j, x_l) = K/2 \cdot (1 - x_j^2)x_l$. This is very close to the desired form where the only thing missing is that the self dynamics are node dependent ($F_j(x_j) = F(x_j)$). We should, despite this, still try for a 1D effective equation that describes the system using Gao's framework. Let us simply differentiate the definition of the effective parameter.

$$\dot{x}_{\text{eff}} = \frac{1}{N}\sum_{j=1}^{N}\dot{x}_j \tag{8.23}$$

$$= \frac{1}{N}\sum_{j=1}^{N}\big(i\omega_j x_j + \frac{Kx_{\text{eff}}}{2}(1 - x_j^2)\big) \tag{8.24}$$

We should keep track of the error in order to keep going without losing too much information when applying approximations. Defining δ_j so that $x_j = x_{\text{eff}} - \delta_j$,

$$\dot{x}_{\text{eff}} = \frac{i}{N}\sum_{j=1}^{N}\omega_j x_j + \frac{K x_{\text{eff}}}{2N}\sum_{j=1}^{N}(1 - x_j^2) \tag{8.25}$$

$$= i\bar{\omega}x_{\text{eff}} - \frac{i}{N}\sum_{j=1}^{N}\omega_j\delta_j + \frac{K x_{\text{eff}}}{2N}\sum_{j=1}^{N}\left(1 - (x_{\text{eff}} - \delta_j)^2\right) \tag{8.26}$$

where $\bar{\omega} = 1/N \cdot \sum_{j=1}^{N}\omega_j$ is the average of the frequencies ω.

$$\dot{x}_{\text{eff}} = i\bar{\omega}x_{\text{eff}} + \frac{K x_{\text{eff}}}{2}(1 - x_{\text{eff}}^2) - \frac{i}{N}\sum_{j=1}^{N}\omega_j\delta_j - \frac{K x_{\text{eff}}}{2N}\sum_{j=1}^{N}\delta_j^2 \tag{8.27}$$

So for small errors δ we throw away any higher order terms and get

$$\dot{x}_{\text{eff}} = i\bar{\omega}x_{\text{eff}} + \frac{K x_{\text{eff}}}{2}(1 - x_{\text{eff}}^2) - \frac{i}{N}\sum_{j=1}^{N}\omega_j\delta_j, \tag{8.28}$$

by only keeping first order terms in the error δ. In the limit $\delta \to \mathbf{0}$ the one dimensional effective equation becomes

$$\dot{x}_{\text{eff}} = i\bar{\omega}x_{\text{eff}} + \frac{K x_{\text{eff}}}{2}(1 - x_{\text{eff}}^2) \tag{8.29}$$

where we should note that the effective parameter β_{eff} we had before is now equal to 1 as we have all to all coupling with a constant coupling strength.

We now turn to the rotating frame of reference where $\hat{x}_{\text{eff}} \equiv x_{\text{eff}}e^{-i\bar{\omega}}t$ so that

$$\dot{\hat{x}}_{\text{eff}} = \frac{\mathrm{d}}{\mathrm{d}t}(x_{\text{eff}}e^{-i\bar{\omega}t}) = \dot{x}_{\text{eff}}e^{i\bar{\omega}t} - i\bar{\omega}x_{\text{eff}}e^{i\bar{\omega}t} \tag{8.30}$$

and we obtain a differential equation for $\hat{x}_{\text{eff}}$ in the form of

$$\dot{\hat{x}}_{\text{eff}} = \frac{K}{2}\hat{x}_{\text{eff}}(1 - \hat{x}_{\text{eff}}^2 e^{2i\bar{\omega}t}) \tag{8.31}$$

where we find stationary points at $\hat{x}_{\text{eff}} = 0$ and $\hat{x}_{\text{eff}} = \pm e^{-i\bar{\omega}t}$. The fixed point at 0 has eigenvalue $K/2$ and is unstable. The other fixed points have negative eigenvalues of $-K$, which makes them stable equilibria. These points translate to fixed points for x_{eff} at $x_{\text{eff}} = 0$ and $x_{\text{eff}} = \pm 1$.

The physical meaning for these is that the order parameter has, as expected, real fixed points. The fixed point where $x_{\text{eff}} = 0$ corresponds to a non-coherence state where the oscillators are distributed equally over phase space. We expect this state to be unstable because a small perturbation in this symmetry would cause for the oscillators to be attracted in the direction of the perturbation even more. The state where $x_{\text{eff}} = 1$ corresponds to complete synchronization. All the phases add up in Eq. (8.16) when we let time run.

Interesting would be to investigate what happens to the synchronization and the resilience of the model if we add a static phase θ_0 in the coupling term in Eq. (8.1) so that the coupling term becomes $\hat{G}(\theta_i, \theta_j) = sin(\theta_i - \theta_j + \theta_0)$. Surprisingly, we will see this in the following chapter when investigating arrays of Josephson junctions.

Chapter 9

Josephson Junctions and Synchronization

Next we will turn our focus towards the Josephson junction. A Josephson junction consists of two superconducting plates with a thin insulator in between them. The Josephson effect can be witnessed in this configuration, a supercurrent can flow from one superconductor to the other without feeling any resistance. Often Josephson junctions are connected in parallel with other electrical components such as resistors, capacitors and inductors. We will first concentrate on a single Josephson junction. The governing equations are

$$V(t) = \frac{\hbar}{2e}\frac{\mathrm{d}\phi}{\mathrm{d}t} \tag{9.1}$$

$$I(t) = I_c \sin(\phi) \tag{9.2}$$

where $V(t)$ is the externally applied voltage over the junction, $I(t)$ the current through the junction, I_c the critical current of the junction and $0 \leq \phi < 2\pi$ the phase difference across the junction. For a DC voltage V_0 we get that the phase difference across the voltage goes linear with time and assumes all of its possible values. Phase space is a cylinder, $0 \leq \phi < 2\pi$,$\infty < \dot{\phi} < \infty$. The DC voltage results in a constant change of phase, thus giving a perpendicular cross section of the phase space. With $\phi = \frac{V_0 2e}{\hbar}t + \phi_0$ and $I = I_c \sin(\frac{V_0 2e}{\hbar}t)$.

This is all very interesting, but what is perhaps more interesting is what happens when we add an extra electrical component. When we add a resistor in parallel with the Josephson junction, as shown below,

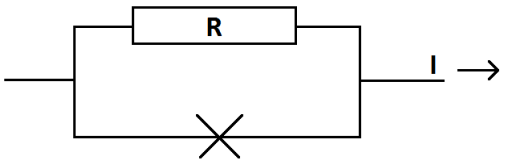

Figure 9.1: A Jospehson junction in parallel with a resistor of resistance R, with external current I.

we can use the Kirchhoff equations to obtain

$$I = I_J + I_R = I_c \sin(\phi) + \frac{V}{R} \tag{9.3}$$

$$= I_c \sin(\phi) + \frac{\hbar}{2eR}\dot{\phi} \tag{9.4}$$

where R is the resistance of the resistor, I_J the current through the Josephson junction and I_R the current through the resistor. This is a first order nonlinear differential equation for ϕ.

To obtain a second order derivative, an electrical component that relates the current to the derivative of the voltage is used.

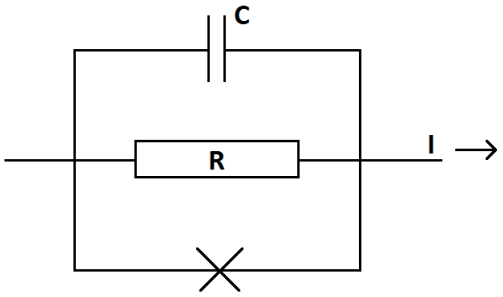

Figure 9.2: A Josephson junction in parallel with a resistor of resistance R and a capacitor with capacitance C, with external current I.

Adding a capacitor in parallel with the junction and the resistor we obtain yields this

$$I = I_J + I_R + I_C = I_c \sin(\phi) + \frac{V}{R} + C\dot{V} \tag{9.5}$$

$$= I_c \sin(\phi) + \frac{\hbar}{2eR}\dot{\phi} + \frac{\hbar C}{2e}\ddot{\phi} \tag{9.6}$$

with I_C the current through the capacitor of capacitance C. This equation is similar to that of a damped pendulum [15] with a constant driving force, there the phase ψ of the pendulum is given by

$$\ddot{\psi} + \delta\dot{\psi} + \kappa^2 \sin(\psi) = \frac{K}{I} \tag{9.7}$$

with δ the damping constant, κ the frequency, K the torque acting on the pendulum and I the moment of inertia.

9.1 Resistively Shunted Junctions in a One Dimensional Array

In the context of this research however, it is more interesting to leave the capacitor for now and instead look at an array of Josephson junctions, all of which are individually in parallel with a resistor. Lets also apply a load with a resistor, capacitor and an inductor in series. The setup is schematically drawn below.

This corresponds to the following set of coupled, first order differential equations of the form

$$\frac{\hbar}{2eR}\dot{\psi}_i + I_C \sin(\psi_i) = I - \dot{Q} \tag{9.8}$$

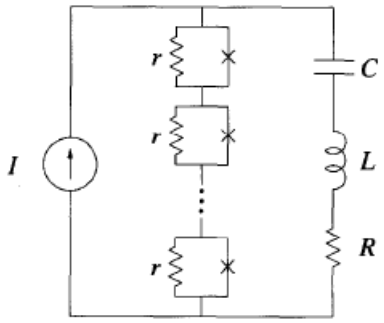

Figure 9.3: An array of Josephson junctions, all separately in parallel with a resistor of resistance r, with external current I and an RLC load. Figure taken from [16] and slightly adapted.

where $\dot{Q}$ is the current through the load. The equations of motions are completed by equating the voltage over the load and the voltage over the array of junctions

$$L\ddot{Q} + r\dot{Q} + \frac{Q}{C} = \frac{\hbar}{2e}\sum_{i=1}^{N}\dot{\psi}_i \tag{9.9}$$

switching to a uniformly rotating phase [17] in the shape of

$$\phi_i = 2\arctan\left(\sqrt{\frac{I-I_C}{I+I_C}}\tan\left(\frac{\psi_i}{2}+\frac{\pi}{4}\right)\right) \tag{9.10}$$

Pikovski [15] derives a differential equation for these phases

$$\dot{\phi}_i = \omega_0 + \frac{\epsilon}{N}\sum_{j=1}^{N}\sin(\phi_j - \phi_i - \alpha) \tag{9.11}$$

where ω_0 would be the rotational frequency if no coupling would be present, ϵ is given as

$$\epsilon = N\frac{2eR^2I\omega_0/\hbar - R\omega_0^2}{\sqrt{(1/C + L\omega_0^2)^2 + (r+NR)^2\omega_0^2}}$$

and alpha is implicitly given as

$$\cos(\alpha) = \frac{L\omega_0^2 - 1/C}{\sqrt{(1/C - L\omega_0^2)^2 + (r+NR)^2\omega_0^2}}. \tag{9.12}$$

The system has been thoroughly investigated [18, 19, 16]. We will however turn to the effective parameter to see whether this displays the same criteria for synchronization.

Let us once again introduce the order parameter, as in the previous section, $re^{i\bar{\phi}}$ given by

$$re^{i\bar{\phi}} = \frac{1}{N}\sum_{j=1}^{N}e^{i\phi_j} \tag{9.13}$$

and variables x_j where

$$x_j \equiv e^{i\phi_j}, \tag{9.14}$$

$$\dot{x}_j = i x_j \dot{\phi}_j = i\omega_0 x_j + \frac{\epsilon r}{2}(e^{-i\alpha} - e^{i\alpha} x_j^2) \tag{9.15}$$

so that for $\bar{\phi} = 0$

$$r = \frac{1}{N}\sum_{j=1}^{N} x_j \tag{9.16}$$

where r is now again the effective parameter in the sense of Gao's framework. A differential equation for r is easily obtained by differentiating the x_j's

$$\dot{r} = i\omega_0 r + \frac{\epsilon r}{2}(e^{-i\alpha} - e^{i\alpha} r^2 - e^{i\alpha}\sum_{j=1}^{N} \delta_j^2) \tag{9.17}$$

Here we use a transformation to a constantly rotating frame of reference and we take the limit of $\delta \to \mathbf{0}$

$$\hat{r} = r e^{-i\omega_0 t} \tag{9.18}$$

so that this has the property

$$\dot{\hat{r}} = \frac{\epsilon \hat{r}}{2}(e^{-i\alpha} - e^{i(\alpha+2\omega_0 t)}\hat{r}^2) \tag{9.19}$$

and we find fixed points at $\hat{r} = 0$ with eigenvalue $\epsilon e^{i\alpha}/2$ and $\hat{r} = \pm e^{-i(\alpha+\omega_0 t)}$ with eigenvalue $-\epsilon e^{i\alpha}$. The stability criteria for the coherent and incoherent states thus depend on the sign of $\epsilon\cos(\alpha)$, as was also found separately [17]. By definition of α in Eq. (9.12) we find that $\|\omega_0\| < 1/\sqrt{LC}$ has to hold in order for the coherent state to be stable.

Chapter 10

Conclusions

At the beginning of this work, in chapter 2, the problem at hand was explained and the derivation of Gao's mean field approximation was shown. It was then argued that the assumptions on the self-dynamics and the interaction term were not trivially satisfied and a more thorough analysis of the error should be formulated. This was done in chapter 3, where a differential equation of the effective node and of the error were both derived. These can both be solved, be it numerically, after which the results can be used to solve the now uncoupled system of equations that remain.

In chapters 4 and 5 we have seen that in the case of the plants and pollinators, the effective equation describes the average behaviour very well as long as $beta_{\text{eff}}$ is far away from its critical value. The region around the critical value of β_{eff}, however, is the interesting region. It is the region where the equilibrium behaviour of the system suddenly changes as the amount of fixed points of the effective equation changes at the critical value of the effective parameter. Moreover, the formalism fails to predict the correct behaviour around the critical value when noise is added to the system. When the system is pushed to the high equilibrium state by the noise, the effective equation predicts that this does not happen, a serious shortcoming. This behaviour is also expected to get worse as the size of the network increases since the "effective" noise, which is a weighted average of the noises on each node, will cancel out even more.

The equilibria of the low dimensional systems that were analyzed in chapter 6 give insight as to why the mean field approximation works in those cases. As expected (because of the all to all coupling), the stable fixed points are both in-phase solutions, resulting in a perfect prediction by the mean field approximation. It would be interesting to see how this develops as the dimension of the system increases and the interactions are no longer as simple as was assumed in this research. This is however increasingly harder to calculate or even display this as the amount of dimensions increases.

As for the Generalized Lotka-Volterra model, it was shown that the mean field approximation might give a wrong indication of the network dynamics. Even when the system has no stable fixed point, the effective equation always seems to find one, regardless of the network topology.

In chapter 8 the formalism was applied to the Kuramoto model. It correctly predicted a coherent and incoherent state but did not take into account the difference in self-dynamics of the oscillators while doing so. We should note that the Kuramoto model is not in the assumed form where the self-dynamics of the nodes are not node dependant. Since the mean field approximation assumes an average drift velocity of each node, it predicts either a fully coherent, or fully incoherent stationary state.

Finally, when applying the theory to an array of resistively shunted Josephson junctions, the formalism correctly predicts the stationary states. It also finds the correct stability criteria, depending on the sign of $\cos(\alpha)$. For this final application the theory seems to work very well.

References

[1] Jianxi Gao, Baruch Barzel, and Albert-László Barabási. "Universal resilience patterns in complex networks." In: *Nature* 530 (7590 2016), pp. 307–312. DOI: 10.1038/nature16948.

[2] Pablo Kaluza et al. "The complex network of global cargo ship movements". In: *Journal of The Royal Society Interface* 7.48 (2010), pp. 1093–1103. ISSN: 1742-5689. DOI: 10.1098/rsif.2009.0495. eprint: http://rsif.royalsocietypublishing.org/content/7/48/1093.full.pdf. URL: http://rsif.royalsocietypublishing.org/content/7/48/1093.

[3] Sergei Maslov, Kim Sneppen, and Alexei Zaliznyak. "Detection of topological patterns in complex networks: correlation profile of the internet". In: *Physica A: Statistical Mechanics and its Applications* 333 (2004), pp. 529–540. ISSN: 0378-4371. DOI: http://dx.doi.org/10.1016/j.physa.2003.06.002. URL: http://www.sciencedirect.com/science/article/pii/S0378437103008409.

[4] Sui Huang et al. "Cell Fates as High-Dimensional Attractor States of a Complex Gene Regulatory Network". In: *Phys. Rev. Lett.* 94 (12 Apr. 2005), p. 128701. DOI: 10.1103/PhysRevLett.94.128701. URL: https://link.aps.org/doi/10.1103/PhysRevLett.94.128701.

[5] Jose G Venegas et al. "Self-organized patchiness in asthma as a prelude to catastrophic shifts." In: *Nature* 434 7034 (2005), pp. 777–782.

[6] Ron Martin. "Regional economic resilience, hysteresis and recessionary shocks". In: *Journal of Economic Geography* 12.1 (2012), pp. 1–32. DOI: 10.1093/jeg/lbr019. eprint: /oup/backfile/content_public/journal/joeg/12/1/10.1093/jeg/lbr019/2/lbr019.pdf. URL: +%20http://dx.doi.org/10.1093/jeg/lbr019.

[7] Charles Perrings. "Resilience in the Dynamics of Economy-Environment Systems". In: *Environmental and Resource Economics* 11.3 (Apr. 1998), pp. 503–520. ISSN: 1573-1502. DOI: 10.1023/A:1008255614276. URL: https://doi.org/10.1023/A:1008255614276.

[8] Robert M May. "Thresholds and breakpoints in ecosystems with a multiplicity of stable states". In: *Nature* 269.5628 (1977), pp. 471–477.

[9] Reuven Cohen et al. "Resilience of the Internet to Random Breakdowns". In: *Phys. Rev. Lett.* 85 (21 Nov. 2000), pp. 4626–4628. DOI: 10.1103/PhysRevLett.85.4626. URL: https://link.aps.org/doi/10.1103/PhysRevLett.85.4626.

[10] Chengyi Tu et al. "Collapse of resilience patterns in generalized Lotka-Volterra dynamics and beyond". In: *Phys. Rev. E* 95 (6 June 2017), p. 062307. DOI: 10.1103/PhysRevE.95.062307.

[11] Jean-François Arnoldi et al. "Particularity of "Universal resilience patterns in complex networks"." In: *bioRxiv* (2016). DOI: 10.1101/056218.

[12] Uri Alon. *An introduction to systems biology: design principles of biological circuits*. CRC press, 2006.

[13] W. C. (Warder Clyde) Allee. *Principles of animal ecology, by W. C. Allee [and others]*. Philadelphia,Saunders Co., 1949, p. 860. URL: http://www.biodiversitylibrary.org/item/31053.

[14] Juan A Acebrón et al. "The Kuramoto model: A simple paradigm for synchronization phenomena". In: *Reviews of modern physics* 77.1 (2005), p. 137.

[15] Arkady Pikovsky, Michael Rosenblum, and Jürgen Kurths. *Synchronization: a universal concept in nonlinear sciences*. Vol. 12. Cambridge university press, 2003.

[16] Shinya Watanabe and Steven H. Strogatz. "Constants of motion for superconducting Josephson arrays". In: *Physica D: Nonlinear Phenomena* 74.3 (1994), pp. 197–253. ISSN: 0167-2789. DOI: http://dx.doi.org/10.1016/0167-2789(94)90196-1.

[17] Kurt Wiesenfeld, Pere Colet, and Steven H. Strogatz. "Synchronization Transitions in a Disordered Josephson Series Array". In: *Phys. Rev. Lett.* 76 (3 Jan. 1996), pp. 404–407. DOI: 10.1103/PhysRevLett.76.404.

[18] Shinya Watanabe and Steven H. Strogatz. "Integrability of a globally coupled oscillator array". In: *Phys. Rev. Lett.* 70 (16 Apr. 1993), pp. 2391–2394. DOI: 10.1103/PhysRevLett.70.2391.

[19] Hidetsugu Sakaguchi and Yoshiki Kuramoto. "A Soluble Active Rotater Model Showing Phase Transitions via Mutual Entertainment". In: *Progress of Theoretical Physics* 76.3 (1986), pp. 576–581. DOI: 10.1143/PTP.76.576.